Behavioral/Systems/Cognitive

Functional Gradients of Auditory Sensitivity along the Anterior Ectosylvian Sulcus of the Cat

Liora Las,[1] Ayelet-Hashahar Shapira,[1] and Israel Nelken[1,2]

[1]Department of Neurobiology, The Alexander Silberman Institute of Life Sciences, and [2]The Interdisciplinary Center for Neural Computation, Hebrew University, Jerusalem 91904, Israel

Determining the spatial direction of sound sources is one of the major computations performed by the auditory system. The anterior ectosylvian sulcus (AES) of cat cortex is known to be important for sound localization. However, there are contradicting reports as to the spatial response properties of neurons in AES: whereas some studies found narrowly tuned neurons, others reported mostly spatially widely tuned neurons. We hypothesized that this is the result of a nonhomogenous distribution of the auditory neurons in this area. To test this possibility, we recorded neuronal activity along the AES, together with a sample of neurons from primary auditory cortex (A1) of cats in response to pure tones and to virtual acoustic space stimuli. In all areas, most neurons responded to both types of stimuli. Neurons located in posterior AES (pAES) showed special response properties that distinguished them from neurons in A1 and from neurons in anterior AES (aAES). The proportion of space-selective neurons among auditory neurons was significantly higher in pAES (82%) than in A1 (72%) and in aAES (60%). Furthermore, whereas the large majority of A1 neurons responded preferentially to contralateral sounds, neurons in pAES (and to a lesser extent in aAES) had their spatial selectivity distributed more homogenously. In particular, 28% of the space-selective neurons in pAES had highly modulated frontal receptive fields, against 8% in A1 and 17% in aAES. We conclude that in cats, pAES contains a secondary auditory cortical field which is specialized for spatial processing, in particular for the representation of frontal space.

Key words: **auditory cortex; anterior ectosylvian sulcus; sound localization; HRTF; electrophysiology; cat**

Introduction

Sound localization is a major computational task of the auditory system. Physical cues for sound localization are extracted by specialized brainstem circuits (Yin, 2002). In mammals, an auditory space map is present in the deep layers of the superior colliculus (King and Palmer, 1983; Middlebrooks and Knudsen, 1984; King, 1993). This space map is synthesized at least to some degree using inputs from lower auditory stations (Schnupp and King, 1997).

In addition to the subcortical circuits, cortical processing has been shown to play an important role in spatial localization. Lesion studies in animals have indicated that an intact auditory cortex is required for fine sound localization [ferrets (Kavanagh and Kelly, 1987; Heffner and Heffner, 1990); cats (Beitel and Kaas, 1993); primates (Heffner, 1997)]. More recent inactivation studies in cats suggested that a number of cortical areas contribute to sound localization behaviors: primary auditory cortex (A1), posterior auditory field (PAF), dorsal zone (DZ), and the anterior ectosylvian sulcus (AES) (see Fig. 1*A*), a multimodal cortical region that contains an auditory field (Jiang et al., 2002; Malhotra et al., 2004; Lomber et al., 2007).

The AES seems particularly important for sound localization because it is the only auditory cortical area that sends heavy projections into the deep layers of the superior colliculus (Meredith and Clemo, 1989). The auditory field in AES was located in the posterior part of the sulcus by Meredith and Clemo (1989) based on the predominance of auditory neurons in that area. However other studies have reported auditory responses from more anterior locations in AES as well (Clarey and Irvine, 1986; Korte and Rauschecker, 1993; Middlebrooks et al., 1998; Jiang et al., 2000).

Although the importance of AES for sound localization is generally accepted, reports of neural responses in AES have shown a large variability. Korte and Rauschecker (1993) reported a population of neurons that had relatively narrow spatial tuning. Furthermore, they demonstrated that in cats deprived from vision after birth, spatial tuning of AES neurons was narrower compared with control animals. This improvement was accompanied by an increase in the percentage of space selective neurons relative to normal cats (from 56 to 86%). Other authors, however, found that most AES neurons had relatively broad spatial receptive fields, with only a small proportion of neurons showing preference to central locations (Middlebrooks et al., 1994, 1998; Jiang et al., 2000).

Some of the reported differences between these studies could result from different recording locations. Therefore, to clarify the

Received Oct. 5, 2007; revised Feb. 12, 2008; accepted Feb. 28, 2008.

This work was supported by grants administered by the United States–Israel Binational Foundation, the Israeli Science Foundation, and the German-Israeli Foundation. We thank M. Long, U. Rokni, and N. Ulanovsky for critical comments. We thank E. D. Young (Johns Hopkins University, Baltimore, MD) for the HRTF set.

Correspondence should be addressed to Israel Nelken, Department of Neurobiology, Hebrew University, Jerusalem 91904, Israel. E-mail: israel@cc.huji.ac.il.

L. Las's present address: McGovern Institute for Brain Research, Department of Brain and Cognitive Sciences, Massachusetts Institute of Technology, Cambridge, MA 02139.

DOI:10.1523/JNEUROSCI.4539-07.2008

 0270-6474/08/283657-11$15.00/0

role of AES in sound processing, we have examined the responses of auditory neurons along the longitudinal axis of AES to pure tones and virtual-space sounds. For comparison purposes we included also a large sample of neurons in A1. We demonstrate a gradient of spatial selectivity along the AES, with the posterior part having an appreciable number of neurons with restricted, frontal spatial tuning. These results may account for the discrepancies between previous studies of AES, and suggest a specific role for posterior AES (pAES) in coding of frontal space.

Materials and Methods

Animal preparation. Experiments were performed on 17 adult cats. All experiments were approved by the animal use and care committee of the Hebrew University Hadassah Medical School. Anesthesia was induced with ketamine (100 mg, i.m.) and with either xylazine (0.1 mg, i.m.) or medetomidine (Domitor, 0.2 mg, i.m.). The trachea was cannulated, and anesthesia was maintained with halothane (0.2–1.5% as needed) mixed with oxygen and nitrous oxide (O_2/N_2O, 30%/70%). Some cats received 0.1 mg atropine sulfate or atropine methyl nitrate (i.m.). A cannula in the radial vein was used to infuse lactated ringer (10–50 ml/h, depending on the condition of the cat) and a cannula in the femoral artery was used to monitor blood pressure. Bicarbonate solution (8.4%, ~5 ml/8 h) was injected (i.v.) to counteract the acidosis that invariably developed during the long recording times (up to 72 h). End-expiratory CO_2 level was kept at ~3%, reducing respiratory drive and thus allowing respiration without the need for pharmacological muscle relaxants.

The temporal muscles were retracted to uncover the skull and the external auditory meati on both sides. The bullas were vented with a 30 cm polyethylene tube (PE 90) to avoid the buildup of pressure in the middle ear, which might result in thresholds shifts. The skull was opened above the suprasylvian sulcus and the craniotomy contained the superior tip of the anterior ectosylvian sulcus, to ensure access to the posterior parts of the AES that lie underneath the middle ectosylvian gyrus. The dura was left intact. Heart rate, breathing rate and quality, CO_2 levels, and body temperature (kept around 38°C using a heating pad) were continuously monitored. Small electrolytic lesions were made at the end of some tracks, to facilitate the reconstruction of the electrode tracks (5–10 μA for 5–10 s). The cats were killed (pentobarbital 50–100 mg, i.v.) and perfused transcardially with saline followed by 500 ml of 4% formaldehyde. Coronal sections (50 μm) of the brains were cut and stained with cresyl violet. All of the data presented here was recorded in penetrations that could be identified and reconstructed.

Electrical recordings. Extracellular recordings were performed in A1 and in AES of the left cerebral hemisphere using two to four glass-coated tungsten electrodes, each of which could be individually driven (EPS; Alpha Omega, Nazareth, Israel). The electrode tips were positioned on the lateral lip of the suprasylvian sulcus and then driven vertically down to access the AES at different locations along its longitudinal axis (Fig. 1). Spikes were sorted using on-line template-based spike sorters (MSD; Alpha Omega). To monitor the quality of the spike sorting, the sorters supply a histogram of the squared error between the detected spikes and the template. When these histograms had a peak followed by a clear minimum, signifying the presence of a homogeneous class of spike shapes similar to the template, the spikes were considered as well separated, representing the activity of a single neuron (for more details on spike sorting, see Moshitch et al. 2006). Only well separated neurons are analyzed here.

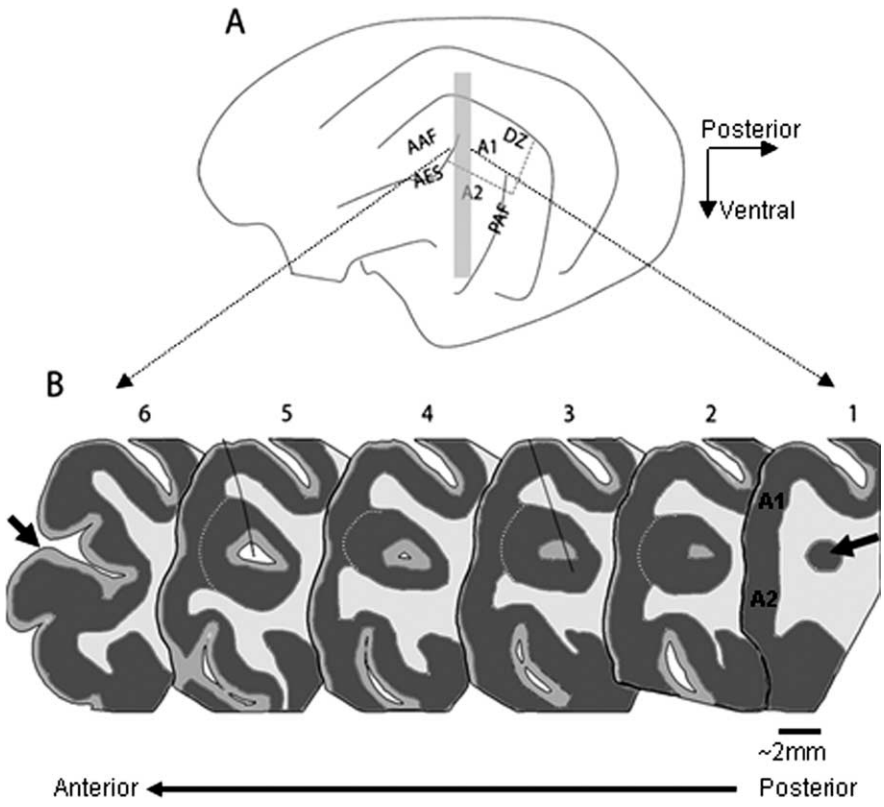

Figure 1. Anatomy of the anterior ectosylvian sulcus. ***A***, Schematic diagram depicting the lateral view of the cat's left hemisphere, including the main cortical auditory areas: A1, A2, the anterior auditory field (AAF), the PAF, the DZ and the AES. ***B***, Schematic representation of six coronal sections from different locations along the longitudinal axis of the AES (the approximate location of these sections is indicated by the gray rectangle in ***A***). The arrow in section 1 indicates the posterior pole of the AES, which consists of a small cluster of cells that increases in size more rostrally, and which lies underneath the auditory fields of A1 and A2. Dark gray corresponds to gray matter, and white corresponds to white matter, whereas intermediate gray represents layer I, a region poor in cells that appears in the middle of the cell cluster forming the posterior pole of AES. The pAES is defined as the part of AES that lies buried underneath the middle ectosylvian gyrus (sections 1–5), and aAES is the open part of the sulcus (represented here by section 6, with the sulcus lips anterior to the opening depicted by an arrow). The white dashed line on sections 2–5 is indicating layer 5, the border between the gray matter of AES and that of A1 and A2. The black lines that partially cross sections 3 and 5 indicate two electrode penetrations that were reconstructed in this brain.

Sound generation. Pure tone stimuli were generated digitally (AP2; Tucker-Davis Technologies, Alachua, FL), converted to analog voltage (DA3-4; Tucker-Davis Technologies), attenuated (PA4 or PA5; Tucker-Davis Technologies) and switched with onset and offset ramps of 10 ms (SW2; Tucker-Davis Technologies). Virtual acoustic stimuli were synthesized off-line (see below) and played from computer files. The sounds were presented to the animal through sealed earphones (designed by G. Sokolich, Custom Sound Systems, Newport Beach, CA), with calibration performed *in situ* by probe microphones (Knowles, Itasca, IL) precalibrated relative to a 1/4 inch (Brüel & Kjaer, Naerum, Denmark) microphone.

Stimulation protocol. After a unit was separated from the background activity, frequency response area (FRA) was measured (45 frequencies, logarithmically spaced between 0.1 and 40 kHz at 8 or 11 sound levels linearly spaced between 0 and 90 dB sound pressure level (SPL), 115 ms long at 1 stimulus/s, each stimulus was presented once). In approximately one-half the units (182 of 377 neurons), a second tone nominally at best frequency was presented starting 70 ms after tone onset. Although the purpose of the second tone was to measure inhibitory sidebands, its settings (frequency and level) were very often inappropriate. Therefore, in all cases in which a second tone was presented, only the first 70 ms of the responses are analyzed here. The best frequency and minimal thresh-

Table 1. Responses to pure tone stimuli

	A1	pAES	aAES
Total number of neurons tested with pure tones	123	126	128
Responsive neurons	74 of 123 (60%)	93 of 126 (74%)	80 of 128 (62%)
Selective neurons	41 of 74 (55%)	56 of 93 (60%)	34 of 80 (42%)

Responsive neurons had significantly larger spike counts after tone onset compared with spike counts for the same time interval preceding tone onset ($p < 0.05$, paired t test). Selective neurons had significant effect of frequency on spike counts (combined across levels at each frequency, one-way ANOVA, $p < 0.05$). For additional details, see Materials and Methods.

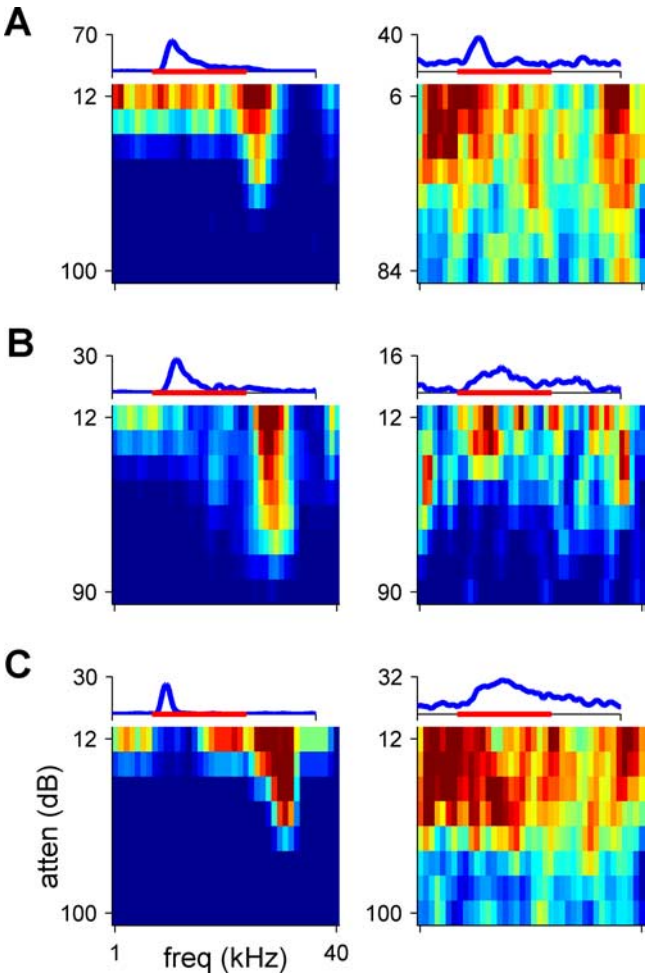

Figure 2. FRAs (color coded) of six representative neurons. The responses in the left column are selective to frequency, whereas the responses in the right column are significant, but nonselective. The PSTH above each FRA represents the firing rate of the neuron, averaged over all stimuli, with the maximum firing rate indicated in spikes per second. The red bar represents the stimulus (115 ms). Note that the abscissa of the FRAs represents frequency, whereas that of the PSTH represents time. ***A***, Two neurons recorded from A1 (color scale saturation, 110 and 26 sp/s). ***B***, Two neurons recorded from pAES (color scale saturation, 44 and 22 sp/s). ***C***, Two neurons recorded from aAES (color scale saturation, 19 and 17 sp/s). Tone levels are expressed in decibel attenuation (atten); 0 dB attenuation is ~100 dB SPL.

old of the neuron were determined. Then, the noise threshold of the neuron was determined using a broad-band noise rate-level function to both ears (15 different levels, covering 88 dB in steps of ~6 dB, 115 ms long with 10 ms linear onset and offset ramps, at 1 stimulus/s). For the rest of the protocol, the noise level was set at ~20 dB above noise threshold.

The spatial sensitivity of a neuron was determined using virtual acoustic space stimuli (VASS) consisting of broad-band noise bursts (100 ms) filtered through nonindividualized head-related transfer functions (HRTFs). HRTFs include all the spatial cues available to an animal (Rice et al., 1995). The VASS covered the frontal region horizontally between −75° to 75° at a resolution of 15°, and vertically between −30° and 30° at a resolution of 7.5°. The preferred location of the neuron was determined in two steps. First, the best azimuth was evaluated in the horizontal midline plane (the elevation was fixed to 0°). Second the best elevation at this azimuth was evaluated. A final set of responses was collected as a function of azimuth along an arc at the best elevation and as a function of elevation along an arc at the best azimuth. Each stimulus was repeated at least 10 times, with interstimulus interval of 1000 ms (onset to onset). All directions were intermixed in a pseudorandom order.

Data analysis. The responses to two types of stimuli, pure tones and VASS, are analyzed here. For each type of stimulus, we distinguish between neuronal responsiveness and neuronal selectivity. Neurons were responsive to a particular stimulus type when they responded significantly (mostly by increasing spike counts) to that stimulus type. Responsive neurons were considered as selective when they showed a significant modulation of their responses as a function of the stimulus parameter.

Responsiveness to pure tones was evaluated by paired t test applied to the spike counts of two equal time windows (70 ms when a second tone was present and 115 ms when there was no second tone) one preceding tone onset and the other after tone onset (Moshitch et al., 2006). Frequency selectivity was evaluated by a one-way ANOVA on spike count of the responses during the time window after stimulus onset. Because each combination of frequency and level was presented only once, the responses to the same frequency were grouped across the different levels. Only responses to levels above minimal threshold were included, except that the responses to tones at the five highest levels were always included.

Responses to the VASS for most neurons were quantified by spike counts measured in a 160 ms time window (from stimulus onset and up to 60 ms after stimulus offset). This rather long time window was selected because some neurons had a significant and long-lasting offset response. Spatial responsiveness of spike counts was evaluated using a paired t test comparing the spike counts in two 160 ms windows, the first preceding stimulus onset and the second after it. The test was performed separately for responses in azimuth and in elevation. Neurons were considered as responsive to space if at least one of the two tests was statistically significant at the 0.05 level. Spatial selectivity was evaluated by a one-way ANOVA test applied to the spike counts, with spatial location as the independent factor. For 35 neurons, spike counts were not selective over the full 160 ms standard response window, but the neurons had significant selectivity when considering either the early response (first 50 ms after stimulus onset, 26 neurons) or the late response (from 50 to 160 ms after stimulus onset, nine neurons). These neurons are analyzed with the rest of the population, considering only the spike counts during the relevant shorter window.

Spatial selectivity was also tested by the first spike latency. Mutual information (MI) between the spatial location of the stimulus and the first spike latency of the responses were computed (Nelken et al., 2005). Only trials that had spikes during a window of 152 ms starting 8 ms after stimulus onset were considered. The mutual information was calculated using the adaptive procedure described by Nelken et al. (2005). We considered the first spike latency to be selective for space when the raw, nonbias corrected MI (that has, up to scaling, a χ^2 distribution under the null hypothesis of no spatial selectivity) was significant at the 0.005 level. This conservative choice was used because the adaptive procedure used to estimate the MI involves multiple comparisons (Nelken et al., 2005).

Classification of spatial tuning curves. spatial tuning curves for spike counts were computed by averaging all the responses in the appropriate response window. Only neurons that showed spatial selectivity were included in this analysis. The tuning curves were classified into two groups according to the modulation depth of the response, defined as the difference between the spike counts at the best and at the worst locations divided by the maximal driven rate. Neurons whose modulation depth was <55% were considered broadly tuned. Neurons with modulation depth >55% were further classified into three laterality groups: contralateral (right), frontal, or ipsilateral (left). We used a procedure whose

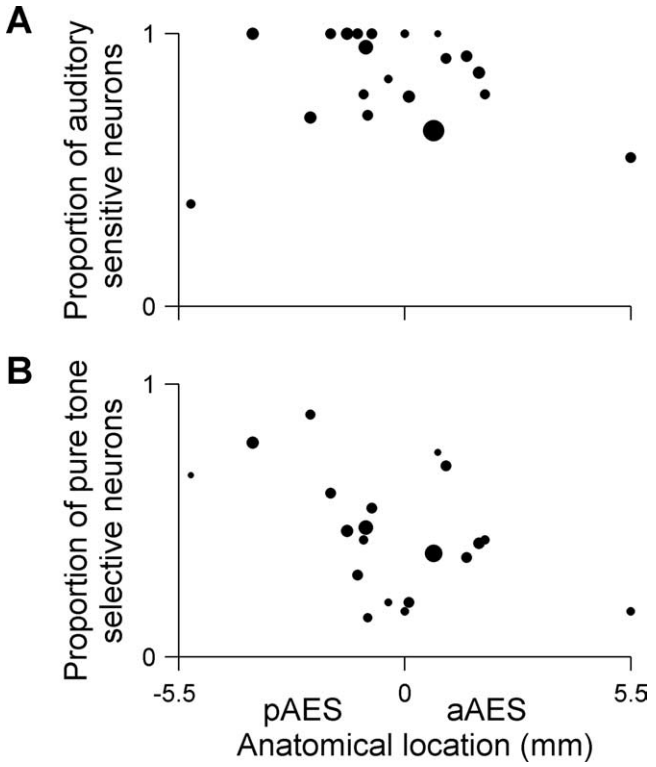

Figure 3. Auditory responsiveness and pure tone selectivity along the AES posterior–anterior axis. ***A***, Auditory responsiveness: each dot represents the proportion of neurons per electrode penetration that responded significantly to one of the auditory stimuli (either pure tone or VASS). The area of each dot is proportional to the total number of neurons that were recorded per electrode penetration. Only penetrations that contained >2 neurons were included (20 penetrations in 11 cats, average of 12.5 neurons per penetration). Auditory responsive neurons were spread equally along the AES ($r = -0.08$, ns). ***B***, Pure tone selectivity: each dot represents the proportion of auditory responsive neurons per electrode penetration that showed pure tone selectivity. Same layout as in Figure 3*A*. Only neurons that were auditory responsive and that were tested with pure tones were included. Only penetrations that contained >2 neurons were included (20 penetrations in 11 cats, average of 10 neurons per penetration). The proportion of frequency-selective neurons decreased along the longitudinal axis of AES ($r = -0.49$, $p < 0.05$).

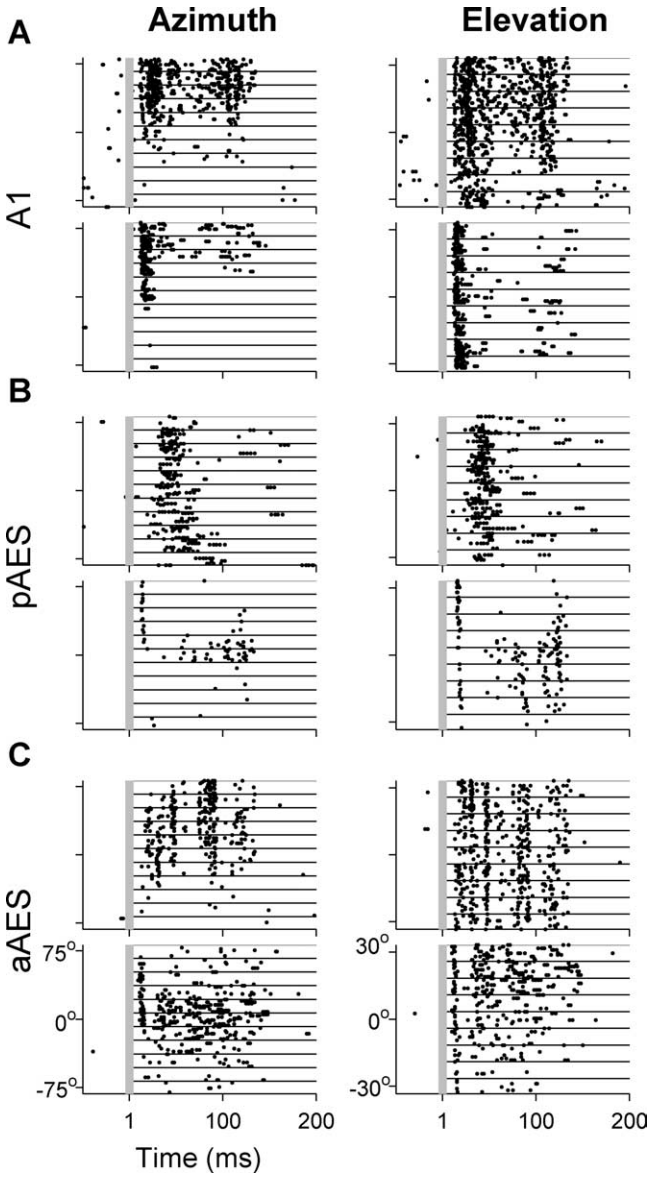

Figure 4. Responses of six representative neurons to VASS. The left column displays the responses to varying virtual azimuths at the best elevation; the right column displays the responses to varying virtual elevations at the best azimuth. Each row illustrates the responses of one neuron. Responses to 10 presentations of each virtual direction are separated by lines. ***A***, Two A1 neurons. ***B***, Two pAES neurons. ***C***, Two aAES neurons. All neurons had significant modulation of both their spike counts and first spike latency as a function of azimuth, except for the bottom neuron in ***A*** that did not have significant modulation of its first spike latency. The bottom example of ***A*** and the top example of ***C*** did not have significant modulation of their spike counts as a function of elevation, and neither example in ***C*** had significant modulation of their first spike latency as a function of elevation.

goal was to use the full shape of the spatial tuning curves for this classification.

We generated a set of tuning curve templates that varied in location and width. The templates were generated from rectangular windows whose widths varied from one to five bins (where one bin corresponds to 15° in azimuth or 7.5° in elevation) and whose location was shifted over the whole range of tested directions. The windows were smoothed by a three-bin triangular window to generate trapezoidal-shaped templates. These templates were evenly divided into contralateral, frontal, and ipsilateral classes according to their location.

For each neuron, the spatial tuning curve was fitted to all templates, by finding the scale and shift of the template that minimized the average squared difference between the spatial tuning curve and the template. The best template (that template that had the least average squared difference of all templates) was selected as the best fit. The neuronal tuning curve was assigned to laterality class of the best template.

Correlation coefficient with anatomical location. The correlation coefficient between the location of the penetrations along the posterior–anterior axis of the AES and the proportion of neurons that responded significantly to the VASS or to pure tone stimuli was calculated by weighting the proportion of responding neurons at each recorded location by the square root of the number of neurons that were recorded at that location. The weights were introduced to account for the differences in the variability in the estimation of the proportions based on different numbers of observations: the confidence in a proportion based on a large number of neurons is higher than on a proportion based on a small number of neurons, and uncertainties in counts are often proportional to their square root (Sokal and Rohlf, 1995).

Statistical tests were considered significant when $p < 0.05$, except for cases in which multiple comparisons were used, in which case we used a more conservative significance level.

Results

We recorded from 123 well separated primary auditory cortex (A1) neurons and from 254 well separated AES neurons. Overall, 79% (97 of 123) of A1 neurons and 81% (206 of 254) of AES neurons showed auditory responsiveness, with significant re-

Table 2. Responses to virtual acoustic space stimuli

	A1	pAES	aAES
Total number of neurons tested with VASS	133	115	140
Space-responsive neurons	94 of 133 (71%)	87 of 115 (76%)	96 of 140 (69%)
Space-selective neurons, spike count only	38	36	34
Space-selective neurons, both spike count and first spike latency	27	33	18
Space-selective neurons, first spike latency only	3	2	5
Overall space selectivity	68 of 94 (72%)	71 of 87 (82%)	57 of 96 (60%)

Space-responsive neurons had significantly larger spike counts after VASS onset compared with spike counts for the same time interval preceding VASS onset ($p < 0.05$, paired t test). Space-selective neurons had significant effect of virtual location on spike counts (one-way ANOVA, $p < 0.05$) or on first spike latency (mutual information between the first spike latency and virtual location). For additional details, see Materials and Methods.

sponses to at least one of the auditory stimuli that were used (pure tones and VASS).

Recording locations

The posterior end of the AES has a complex geometry (Meredith and Clemo, 1989): the ventral and dorsal lips of the sulcus fuse together, forming a closed "sock," which lies underneath, and is sometimes continuous with, the anterior middle ectosylvian gyrus (Fig. 1*A*). The posterior pole of the AES consists of a small cluster of cells which increases in size more rostrally (Fig. 1*B1*, arrow). In most animals, a cortical layer I-like region appears a few hundred microns anterior to the pole, in the middle of the cell cluster (Fig. 1*B2*,*3* intermediate gray), followed by the appearance of a canal (Fig. 1*B4*,*5*, white). On a coronal section, the cortex of the posterior AES and the cortex of the middle ectosylvian gyrus are often continuous along their infragranular layers (Meredith and Clemo, 1989). Finally, the canal underneath the middle ectosylvian gyrus opens, becoming the banks and fundus of the open sulcus (Fig. 1*B6*).

Recordings were made along the longitudinal axis of the AES, in the sock region and in the posterior part of the open sulcus (for the locations of two electrode tracks, see Fig. 1*B3*,*5*). Neurons were divided into those belonging to A1 and those belonging to AES. Because of the dorsoventral orientation of the penetrations, the electrodes usually traversed the white matter before entering the gray matter of the AES. In such penetrations, the sequence of electrode depth readings at the recording locations could be easily interpreted and neurons assigned unambiguously to either A1 or AES. In some cases, the electrodes remained in the gray matter throughout the track, traversing the border region between A1 and the AES cortex. In such cases, we used the prominent layer 5 to separate between A1 and AES (Meredith and Clemo, 1989). More refined determination of the layers in which recordings were made was hard to perform because of the complex geometry of pAES and because of the uncertainty in the correspondence between electrode depth readings and actual location in the histological material.

In addition to the classification into A1 and AES, neurons recorded in AES were classified according to their longitudinal position along the AES. We defined neurons that were located in the open sulcus (as in Fig. 1*B6*) as belonging to the anterior AES (aAES), and neurons that were located in the closed sulcus (Fig. 1*B*, between *1* and *5*) as belonging to the pAES.

Responses to pure tones

Responses to pure tones are the most basic characteristics of auditory neurons, but they have not been quantitatively assessed in most previous studies of neuronal responses in AES (Meredith and Clemo, 1989; Korte and Rauschecker, 1993; Middlebrooks et al., 1998; Xu et al., 1998; Jiang et al., 2000). Neurons responding to pure tones were found in A1, pAES, and aAES (Table 1). Examples of FRAs are displayed in Figure 2. Neurons with sharp, compact tuning (Fig. 2, left column), as well as neurons that had broad, fractured excitatory areas (Fig. 2, right column), were found in each of these three areas (for information regarding such FRAs in A1, see Moshitch et al. 2006).

No correlation was found between the proportion of auditory responsive neurons (neurons that responded significantly to either pure tone or VASS) and their anatomical location along the AES (Fig. 3*A*) ($r = -0.08$, not significant). Furthermore, there were no significant differences between the proportion of neurons that responded significantly to pure tones in A1, pAES, and aAES (Table 1). However, the proportion of frequency-selective neurons (auditory-responsive neurons that showed significant modulation of their firing as a function of frequency, see Materials and Methods) decreased along the longitudinal axis of AES (Fig. 3*B*) ($r = -0.43$, $p < 0.05$, calculated without the rightmost point because of its possible high leverage; the correlation is somewhat higher when using all data, $r = -0.49$, $p < 0.05$). The proportion of frequency-selective responses in pAES (60%) was similar to that in A1 (55%), and was significantly higher than in aAES (42%) ($\chi^2 = 5.4$, df = 1, $p < 0.05$) (Table 1).

Responses to virtual acoustic space stimuli

Figure 4 shows the responses of six neurons to VASS with varying virtual azimuths (left column) and elevations (right column). In all three areas, neurons with reproducible and spatially selective responses could be found. The maximal evoked spike rates in the standard 160 ms window were similar in all three regions, and ranged between 6.25–180 sp/s (spikes per second; ~7 spikes in the 160 ms window on average). The responses could span the whole duration of the stimulus and were not limited to onsets: the median of the maximal evoked spike rates during the first 50 ms of the stimulus was 60 sp/s for A1, pAES, and aAES, and in the next 110 ms of the stimulus it was 36, 36, and 45 sp/s for A1, pAES, and aAES, respectively.

Virtual sound source direction modulated both spike rates and spike patterns, and both changes often co-occurred (Fig. 4). In some neurons, the responses had a nontrivial temporal pattern that was apparent in all responses independent of virtual direction (Fig. 4*C*, top, in response to elevation). Because the same noise segment was used in all VASS, it is probable that such patterns indicate locking to a specific sequence of acoustic events during the stimulus. Unfortunately, the amount of data was not sufficient to unambiguously identify these events. In most neurons, however, the responses did not contain such precise firing patterns, even when the response continued throughout the stimulus (Fig. 4*C*, bottom).

Because both spike rates and temporal response patterns are modulated by virtual direction, testing for spatial selectivity should take into consideration temporal features of the responses. Previous studies have shown that both spike count (Imig et al., 1990; Rajan et al., 1990) and first spike latency (Brugge et al., 1996; Eggermont, 1998; Mickey and Middlebrooks, 2003) carry information about spatial direction. The vast majority of both A1 and AES neurons showed significant modulation of their mean spike counts with virtual direction (>90% of the neurons in each area). Consistently with other

reports, many neurons had significant modulation of their first spike latency with virtual direction (~40% in each area). However, only a small minority (<10% in each area) of the space selective neurons had significant modulation of their first spike latency without having also significant modulation of their spike counts.

Table 2 shows the total number of neurons that were tested with VASS (azimuth, elevation, or both), and the proportions of the neurons that responded significantly to VASS (see Materials and Methods, Space-responsive neurons). No significant difference was found between the proportions of the neurons that responded significantly to the VASS at the three areas (~70% of the neurons in each area). More than one-half the space-responsive neurons were space-selective (as judged by modulation of spike rate or first spike latency) with 72, 82, and 60% of the neurons showing spatial selectivity in A1, pAES, and aAES respectively (these differences were significant: $\chi^2 = 11.1$, df = 2, $p < 0.05$). Thus, neurons in pAES were significantly more likely to show spatial selectivity than neurons in aAES.

The nonhomogeneous distribution of spatial selectivity along the AES was also apparent in the significant correlation between the proportion of space selective neurons and their anatomical location within AES (Fig. 5*A*) ($r = -0.41$, $p = 0.003$). Significant correlations were also obtained when analyzing the selectivity to azimuth and elevation separately. The proportion of azimuth responsive neurons that were selective to azimuth decreased along the posterior–anterior axis of AES (Fig. 5*B*) ($r = -0.53$, $p = 0.0003$). A similar trend, although a weaker one, was observed for the proportion of elevation responsive neurons that were selective to elevation (Fig. 5*C*) ($r = -0.39$, $p = 0.006$). The most posterior point in Figure 5 is relatively distant from the other points and therefore might have high leverage on the correlation coefficients. However, these correlations remained significant even when this point was removed from the calculation (space selectivity, $r = -0.38$, $p = 0.007$; azimuth selectivity, $r = 0.39$, $p = 0.0006$; elevation selectivity, $r = -0.32$, $p = 0.03$).

Because only a small minority of the neurons had space selectivity in their first spike latency without having space selectivity in their spike counts too, for the rest of the study we discuss only the spatial selectivity of spike counts.

In all three anatomical areas, we found space-responsive neurons that did not have space selectivity. Such neurons could be truly omnidirectional, but alternatively they could have weak responses so that the statistical tests were unable to demonstrate a significant effect of stimulus direction on the neuronal responses. To study these possibilities we defined "robust response" as a response whose significance level in the *t* test for spatial responsiveness was better than 0.001, indicating a high signal-to-noise ratio in the responses (the use of significance level to indicate response strength is valid here because all neurons were tested with about the same number of stimulus presentations). We interpret robust responses that lack space selectivity as indicating true omnidirectional responses. Among space-selective neurons, 86% had a robust response by this criterion. Among the space-nonselective neurons, about half (52, 63, and 35% in A1, pAES, and aAES, respectively) had such robust responses. Thus, space-nonselective responses were indeed associated with overall less robust responses to the VASS stimuli. Nevertheless, a substantial number of space-nonselective neurons had robust responses and therefore true omnidirectional responses within the restricted sector of space that was tested here.

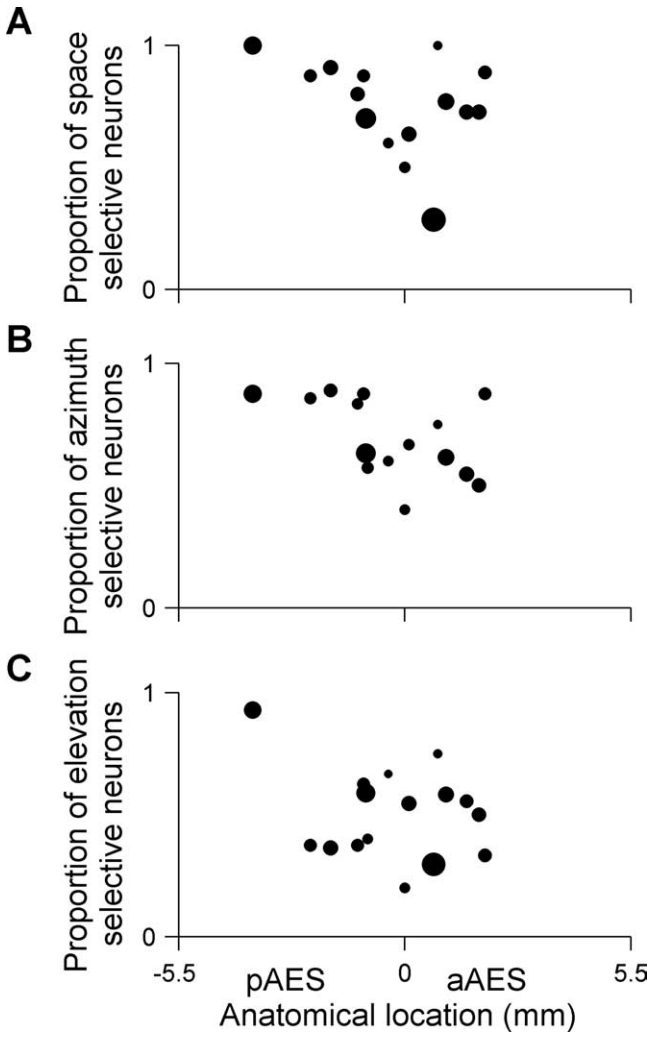

Figure 5. Space selectivity along the AES posterior–anterior axis. ***A***, Space selectivity: each dot represents the proportion of space-responsive neurons that were space-selective in each electrode penetration. Space-responsive neurons were selective to azimuth, to elevation, or to both. The area of each dot is proportional to the total number of neurons that were space-responsive per electrode penetration (16 penetrations in 10 cats, average of 11 neurons per penetration). The proportion of space-selective neurons decreased along the longitudinal axis of AES ($r = -0.41$, $p < 0.05$). ***B***, Azimuth selectivity: each dot represents the proportion of azimuth responsive neurons that were selective to azimuth (15 penetrations in 9 cats, average of 9 neurons per penetration). The proportion of azimuth responsive neurons that were selective to azimuth decreased along the posterior-anterior axis of AES ($r = -0.53$, $p < 0.05$). ***C***, Elevation selectivity: each dot represents the proportion of elevation responsive neurons that were selective to elevation (16 penetrations in 10 cats, average of 10 neurons per penetration). The proportion of elevation responsive neurons that were selective to elevation decreased along the posterior-anterior axis of AES ($r = -0.39$, $p < 0.05$). The total number of penetrations in ***A*** and ***C*** is greater by one from the number of penetrations in ***B*** because in one penetration, only responses to varying elevations were recorded. In all cases, only penetrations with more than two responsive neurons are displayed.

Properties of azimuth and elevation selective neurons

Selectivity to azimuth was more common than selectivity to elevation [36 of 61 (59%), 58 of 77 (75%), and 34 of 57 (60%) for azimuth vs 19 of 46 (41%), 36 of 63 (57%), and 22 of 44 (50%) for elevation in A1, pAES, and aAES respectively; paired *t* test between the log odds, $t = 5$, df = 2, $p < 0.05$].

Figure 6 displays the raster plots of 12 neurons in response to varying virtual azimuths, and the resulting normalized tuning curves. Four neurons are displayed from each area. We first divided the tuning curves into two groups according to their mod-

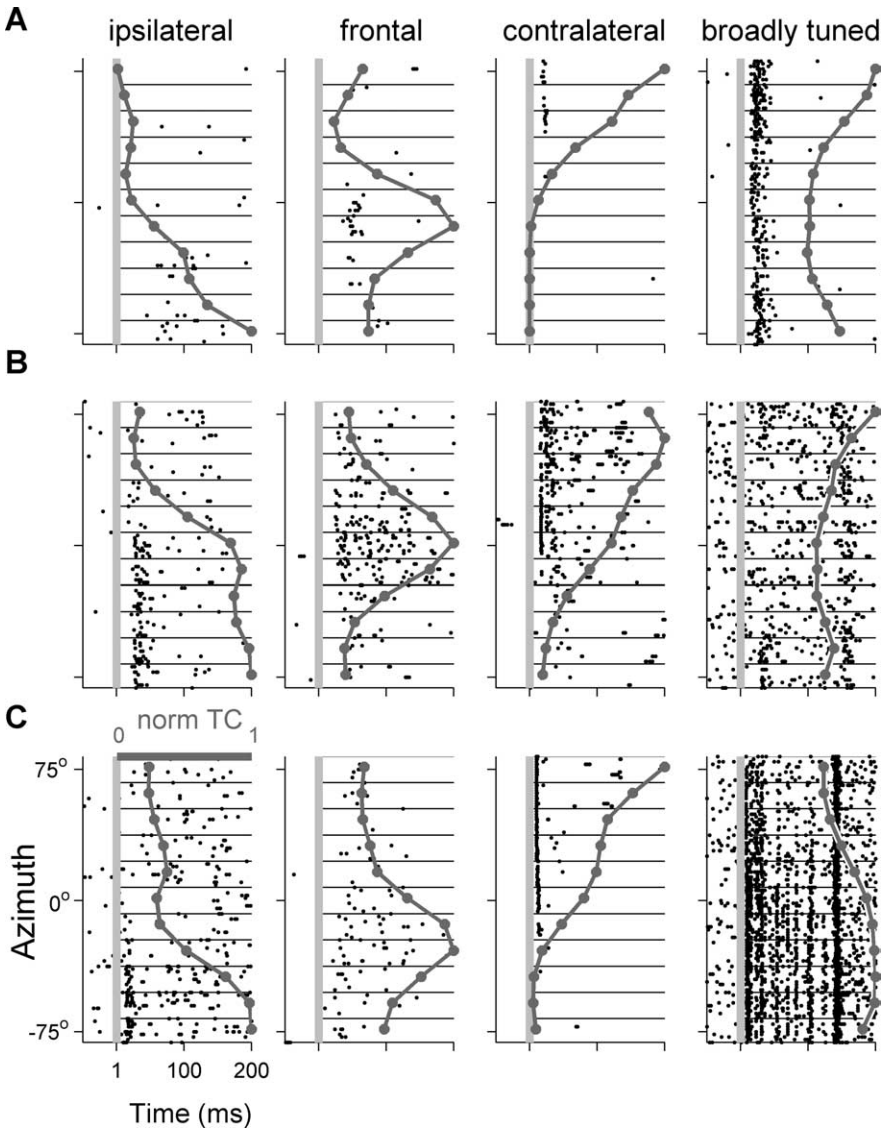

Figure 6. Raster plots and normalized azimuth tuning curves (dark gray line) of 12 spatially selective neurons. The first three columns depict neurons with modulation depths >55%. Preferred azimuth could be ipsilateral (left column), frontal (second column), or contralateral (third column). The rightmost column displays azimuth selective neurons that had modulation depths <55%, considered as broad tuning curves. ***A***, A1. ***B***, pAES. ***C***, aAES.

ulation depth: the difference between the spike counts at the best and at the worst locations. Neurons whose modulation depth was <55% (so that their worst response was larger than 45% of their maximal response) were considered broadly tuned. Broadly tuned neurons were found in each of the three areas: they responded to all tested virtual azimuths, but had significant differences in spike counts between different virtual directions (Fig. 6, right column). The proportion of the azimuth selective neurons having broad tuning curve was significantly different between the three areas, with the smallest proportion found in pAES (14, 2, and 18% for A1, pAES, and aAES, respectively; $\chi^2 = 7.6$, df = 2, $p < 0.05$) (Fig. 7, bottom).

Thus, the majority of the azimuth-selective neurons had modulation depth of >55% (86, 99, and 91% on average in A1, pAES, and aAES, respectively). Preferred azimuths could be ipsilateral (left), frontal, or contralateral (right) (Fig. 6, three left columns). To classify the tuning curves by their preferred azimuth, neural tuning curves were assigned to one of three laterality classes (ipsilateral, contralateral, and frontal), using the fits to model tuning curves (see Materials and Methods) (the same number of model tuning curves were assigned to each class).

A clear difference in the distribution of the best azimuth between the three anatomical areas emerged (Fig. 7). Although most of A1 neurons responded mainly to the contralateral (right) side, pAES had a large number of neurons with frontal spatial tuning curves (28%), almost twice the percentage in aAES (17%), and more than three times the percentage of frontal neurons in A1 (8%). The distributions of laterality classes in pAES and A1 were significantly different ($\chi^2 = 10.6$, df = 3, $p < 0.05$), and so were the differences between pAES and aAES ($\chi^2 = 8.5$, df = 3, $p < 0.05$).

Using other levels of modulation depth for discriminating between broadly tuned neurons and the rest (using values between 40 and 70%) resulted in similar patterns of differences between A1, pAES, and aAES, which however were somewhat weaker and not always significant. The analysis here considered only well separated neurons, but similar proportions were found when including the responses of small multiunit clusters (data not shown).

Similar analysis was performed on the tuning curves of the elevation-selective neurons. Figure 8 shows the responses of nine representative neurons to different virtual elevations; Figure 9 shows the distribution of normalized tuning curves to three model classes of elevation. No clear difference could be observed between the three anatomical areas with respect to the distribution of best elevations. However, it should be noted that the range tested here was only 60°, and tests over larger range of elevations could in principle result in significant differences between the three areas. Consistent with previous reports (Xu et al., 1998; Stecker et al., 2005b) in each of the three areas the majority of the neurons responded mostly to virtual elevations above the horizon.

Comparison between responses to VASS and to pure tones

Most of the space responsive neurons whose FRAs were also available were found to be responsive to pure tones as well (Table 3) [62 of 83 (75%) for A1, 61 of 76 (80%) for pAES, and 67 of 85 (79%) for aAES]. Conversely, an even larger majority of neurons that had significant tone response also had significant responses to the VASS [62 of 70 (89%), 61 of 69 (88%), and 67 of 80 (84%) for A1, pAES, and aAES, respectively]. It should be remembered that the responsiveness test for tones was substantially less powerful than the responsiveness test for VASS, therefore possibly inflating the percentage of neurons in the space-responsive, tone-nonresponsive class. Thus, as a general rule, neurons that responded to any sound responded to both VASS and pure tones. Only a minority, <20% of the neurons, had possibly specific

responses to VASS without significantly responding to pure tones as well.

Discussion

In the present study we examined the neural responses to pure tones and to VASS in A1 and along the longitudinal axis of the AES. Auditory responsiveness in AES was generally as high as in A1. Neurons in pAES were mostly as responsive as neurons in aAES, but they tended to be more selective to stimulus parameters, both frequency and virtual direction.

Methodological issues

The VASS used here were synthesized with nonindividualized HRTFs. Nonindividualized HRTFs might be inappropriate for studying spatial selectivity, because the nervous system presumably adapts to the specific spectral cues imposed by the animal's own ears. However, most available evidence suggest that such effects, even if present, are not large. First, the difference between HRTFs measured from different cats is relatively small (Rice et al., 1992; Young et al., 1996). Second, at least in the ferret A1 it has been shown that spatial responses measured using individual HRTFs or nonindividual HRTFs, although significantly different (Mrsic-Flogel et al., 2001), are nevertheless similar and are essentially fully determined by the acoustic structure of the VASS (Schnupp et al., 2001; Mrsic-Flogel et al., 2003). Third, comparing the spatial tuning of inferior colliculus neurons in barn owl using individual and nonindividual HRTF did not show any appreciable differences (Keller et al., 1998). Fourth, the data reported here from A1 is similar to data collected with free-field stimulation (Mickey and Middlebrooks, 2003) or to studies that used a different set of nonindividualized HRTFs (Brugge et al., 1994, 1998).

We are aware of a single study that reported large differences between spatial receptive fields measured with individualized and nonindividualized HRTFs (Sterbing et al., 2003). This study suggested that the use of nonindividualized HRTFs caused a broadening of the receptive fields and shifted the best direction of their tuning curves away from the midline. Because our main result is the over-representation of frontal space in pAES, such an effect would actually weaken our results, making them conservative, and therefore strengthen our conclusions.

The present experiments were performed under halothane anesthesia. Consistently with previous reports (Moshitch et al., 2006) under halothane the neuronal responses were comparable with the ones reported in awake animals. These included complex and stimulus-sensitive temporal response patterns, and relatively restricted receptive fields. Furthermore, as found in awake cats, most neurons that were space-sensitive had this sensitivity already in their spike counts (Mickey and Middlebrooks, 2003).

Table 3. Responses to VASS versus pure tones

	A1		pAES		aAES	
	Space+	Space−	Space+	Space−	Space+	Space−
Tone+	62	8	61	8	67	13
Tone−	21	26	15	18	18	30

+, Responsive; −, nonresponsive. The definitions of tone- and space-responsive and tone- and space-nonresponsive neurons are as in Tables 1 and 2. For additional details, see Materials and Methods.

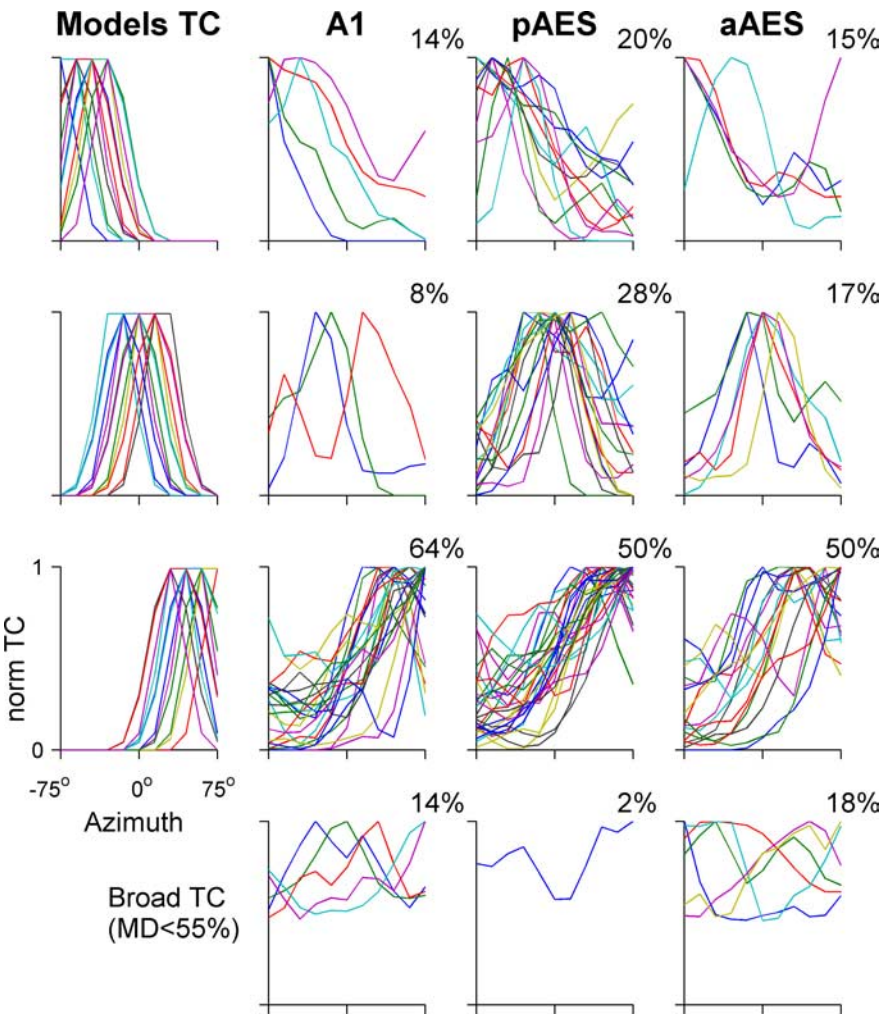

Figure 7. Normalized tuning curves of azimuth selective neurons distributed by laterality. The bottom row displays broad tuning curves of spatially selective neurons with modulation depth <55% in A1, pAES, and aAES. The leftmost column displays the model tuning curves in each laterality class, used for the classification as described in Materials and Methods. The upper three rows display the tuning curves with modulation depths >55% of each laterality class. The proportion of neuronal tuning curves assigned to each class is displayed at each panel. The distributions of laterality classes in pAES and A1 were significantly different, as were the distributions of laterality classes in aAES and pAES.

Functional anatomy of spatial selectivity in A1 and AES

It is well known that neurons in A1 have spatial selectivity (Middlebrooks and Pettigrew, 1981; Imig et al., 1990; Rajan et al., 1990; Poirier et al., 1997). Consistently with these reports, we found that in A1 most of the auditory neurons (72%) showed spatial selectivity to VASS. This percentage is very similar to the percentage reported when using either broadband free field sounds in A1 of awake animals (82%) (Mickey and Middlebrooks, 2003), or nonindividualized HRTFs (79%) (Brugge et al., 1994). Moreover, consistent with previous reports, most of our

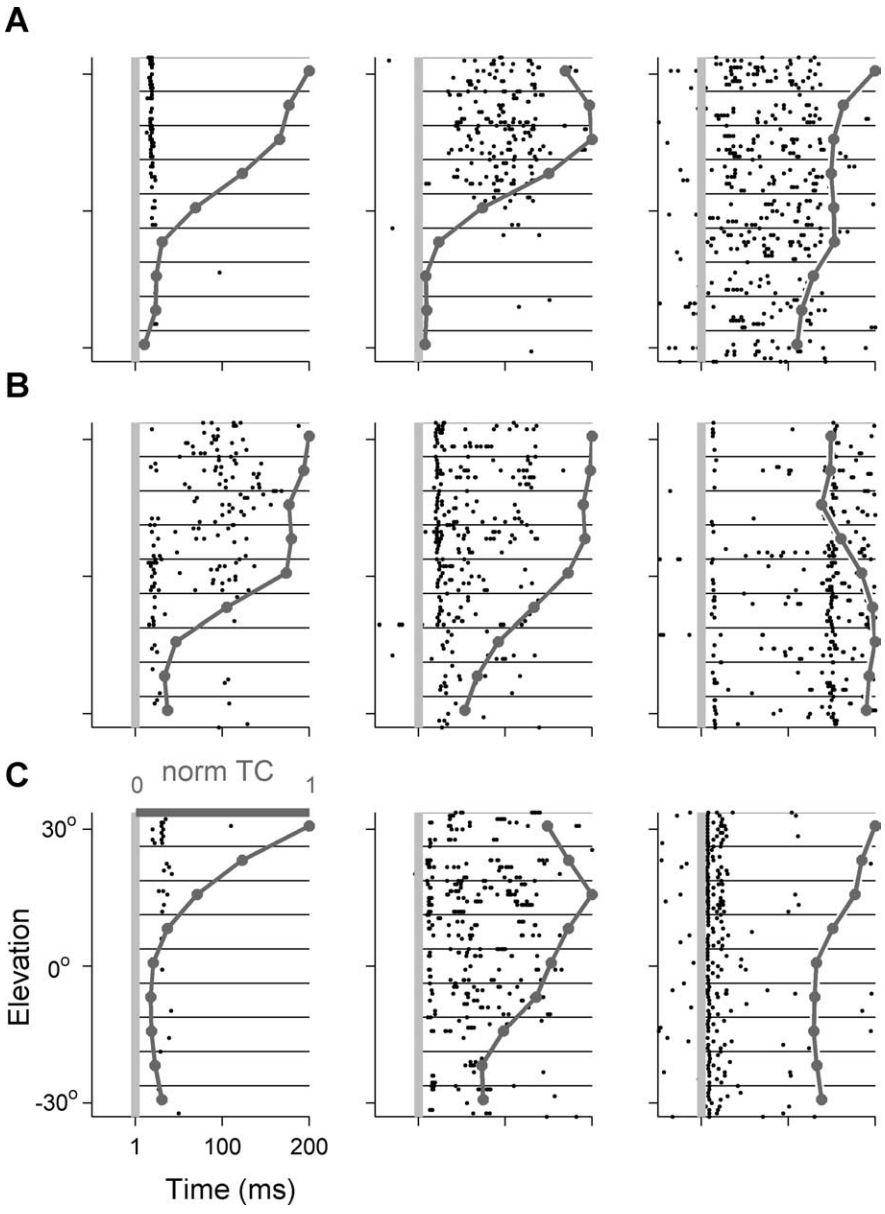

Figure 8. Raster plots and normalized elevation tuning curves (dark gray line) of nine spatially selective neurons. The first two columns display responses of neurons with modulation depths >55%. The rightmost column displays elevation selective neurons that had modulation depths smaller than 55%. ***A***, A1. ***B***, pAES. ***C***, aAES.

space selective neurons in A1 responded best to sound sources located in the contralateral hemifield, and only a small percentage of neurons had their spatial preference in the ipsilateral hemifield or in the frontal area.

In AES, however, our results differ from a number of previous reports. First, the percentage of space-selective neurons reported here in pAES is substantially larger than in previous studies. Jiang et al. (2000) reported that ~50% of their AES responsive neurons showed azimuth preference (excluding neurons that could not be classified). This number is compatible with our aAES data [31 of 57 (54%)], but not with our pAES data [57 of 77 (74%)]. Second, we report here that pAES neurons show a large percentage of ipsilateral and frontal neurons; these seem to be much less prevalent in previous reports [e.g., 2.5% ipsilateral neurons in the study by Jiang et al. (2000) vs 20% here].

Although this discrepancy could be attributable to methodological issues, we believe that the discrepancy reflects differences in the sampling of the different anatomical subdivisions of the AES. Most of the previous studies that reported auditory responses in AES recorded only from the banks and fundus of the open AES, rather than from the "sock" region, which is hidden underneath the medial ectosylvian gyrus. However, Meredith and Clemo (1989) argued that the auditory area within AES lies mostly in the sock region. Our results confirm that auditory responses in AES are not homogenous, with pAES containing more frequency- and space-selective neurons than aAES. Furthermore, we found that space representation in pAES is more homogenous than in aAES and in A1, with ~30% of its spatial selective neurons having close receptive fields with best locations close to the midline compared with 17 and 8% in aAES and A1, respectively.

Our results support the conclusions of Meredith and Clemo (1989) and of Korte and Rauschecker (1993) regarding the presence of a separate auditory field in the sock region of AES. This area has a high concentration of auditory neurons (Table 1). These neurons typically have restricted frequency selectivity (Fig. 3*B*), a large percentage of them is spatially selective (Fig. 5*A*), and they over-represent frontal space relative to A1 and aAES (Fig. 7).

The data presented here suggest that there are rough gradients of these properties along AES, but these gradients are based on pooling data across animals. It may well be that there is a single, homogeneous auditory field in the sock region of AES whose borders are somewhat variable between animals, resulting in the apparent gradients reported here. This field is clearly different from A1 and from the auditory responses in the banks and fundus of the open AES. We propose to reserve the name FAES (Clarey and Irvine, 1986; Meredith and Clemo, 1989) or AEA (Korte and Rauschecker, 1993) specifically to this field.

Consistent with previous studies, our results demonstrate the presence of substantial amounts of auditory responses anterior to the fusion of AES lips, with the most anterior penetration, 5 mm anterior to the fusion point, having >50% auditory neurons (although with weak frequency and spatial selectivity). These auditory responses could correspond to an extension of nearby auditory fields into the sulcus, but the carefully study of Clarey and Irvine (1990a,b) strongly argues against this. Alternatively, there could be a separate auditory field in the open sulcus, or multimodal fields (Meredith and Clemo, 1989). Our results are insufficient for discriminating between these alternatives.

Neuronal codes for sound localization

The spatial tuning curves of single neurons are wider than behavioral spatial acuity. This ubiquitous observation suggests that space is represented by the responses of neuronal populations. The simplest model for population coding assumes the availabil-

ity of a population of relatively narrowly tuned neurons whose best locations span equally all directions in space, enabling the construction of a "population vector" by simple weighted averaging. However, as argued by Middlebrooks and others, this model is not very probable in many cortical stations, because neurons tuned to the front are rare in A1, PAF, DZ, and A2, compared with neurons representing the contralateral hemisphere (McAlpine et al., 2001; Stecker et al., 2003, 2005a). As a result, simple readout mechanisms based e.g., on simple averaging of best directions weighted by firing rates would fail to correctly encode space (although this conclusion is not tight: Jenison and Reale, 2003).

An appealing model for spatial coding in cortex suggested recently, the "opponent model," is based on the comparison of two subpopulations of "panoramic neurons": neurons with preference to contralateral space, and neurons with preference to ipsilateral space (McAlpine and Grothe, 2003; Stecker et al., 2005a). Because lesions in the auditory cortex of one hemisphere cause noticeable deficits of sound localization mainly in the contralateral hemisphere, models using opponent populations require a representation of both hemifields in each hemisphere (Stecker et al., 2005a). The relatively large population of ipsilateral neurons in AES would therefore be useful for opponent models. By the same token, the relatively large population of frontal neurons we found in pAES could serve as a third subpopulation of neurons in a variant of the opponent model (Harper and McAlpine, 2004). Assuming that AES is organized similarly in the two hemispheres, the representation of the frontal area would be double, perhaps improving accuracy around the midline as observed in behaving cats (May and Huang, 1996) and humans (Blauert, 1997). Alternatively, this large frontal population could encode frontal locations using a simple rate code (Korte and Rauschecker, 1993).

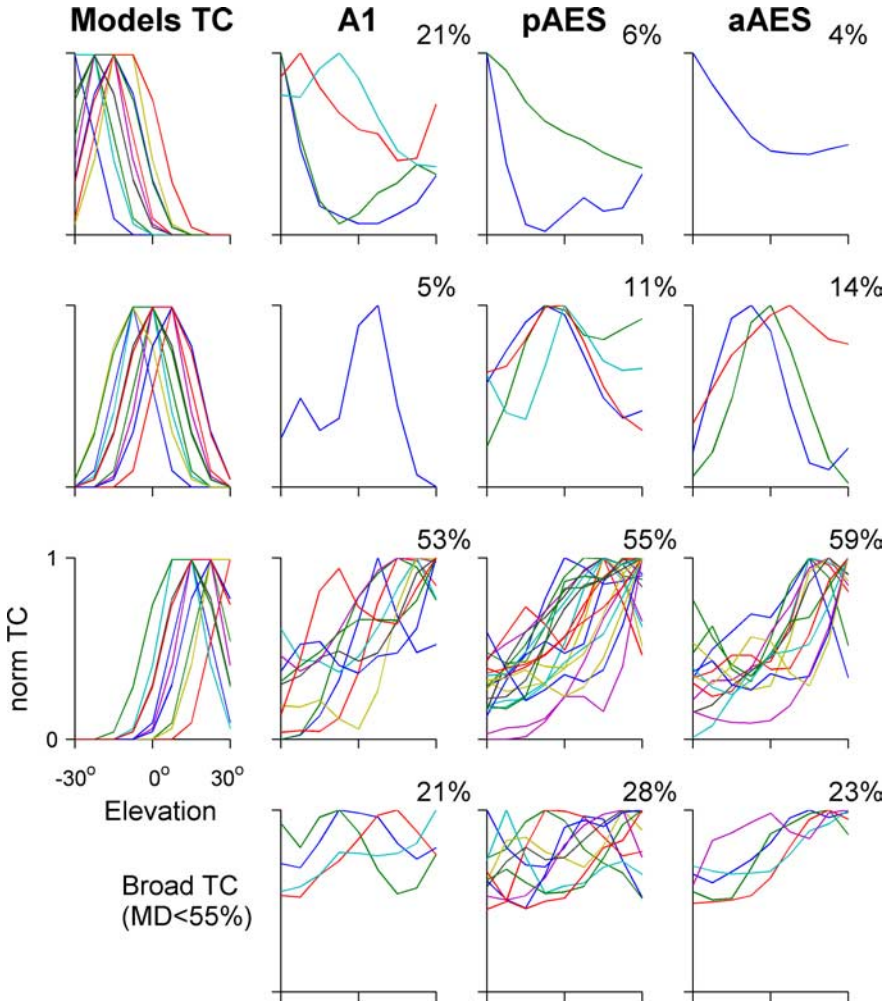

Figure 9. Normalized tuning curves of elevation-selective neurons distributed by elevation preference. Same layout as in Figure 7.

We have shown here that the auditory responses in AES are distributed nonhomogeneously, with the posterior AES showing higher proportion of frequency and space selective neurons compared with the anterior AES. Posterior AES contains the highest proportion of neurons tuned to the front reported in any cat cortical field. We suggest that posterior AES specializes in taking the crudely represented spatial information available in the responses of lower auditory areas, including A1, and re-represent it, with special emphasis on the highly important frontal locations.

References

Beitel RE, Kaas JH (1993) Effects of bilateral and unilateral ablation of auditory cortex in cats on the unconditioned head orienting response to acoustic stimuli. J Neurophysiol 70:351–369.

Blauert J (1997) Spatial hearing. Cambridge, MA: MIT.

Brugge JF, Reale RA, Hind JE, Chan JC, Musicant AD, Poon PW (1994) Simulation of free-field sound sources and its application to studies of cortical mechanisms of sound localization in the cat. Hear Res 73:67–84.

Brugge JF, Reale RA, Hind JE (1996) The structure of spatial receptive fields of neurons in primary auditory cortex of the cat. J Neurosci 16:4420–4437.

Brugge JF, Reale RA, Hind JE (1998) Spatial receptive fields of primary auditory cortical neurons in quiet and in the presence of continuous background noise. J Neurophysiol 80:2417–2432.

Clarey JC, Irvine DR (1986) Auditory response properties of neurons in the anterior ectosylvian sulcus of the cat. Brain Res 386:12–19.

Clarey JC, Irvine DR (1990a) The anterior ectosylvian sulcal auditory field in the cat: I. An electrophysiological study of its relationship to surrounding auditory cortical fields. J Comp Neurol 301:289–303.

Clarey JC, Irvine DR (1990b) The anterior ectosylvian sulcal auditory field in the cat: II. A horseradish peroxidase study of its thalamic and cortical connections. J Comp Neurol 301:304–324.

Eggermont JJ (1998) Azimuth coding in primary auditory cortex of the cat. II. Relative latency and interspike interval representation. J Neurophysiol 80:2151–2161.

Harper NS, McAlpine D (2004) Optimal neural population coding of an auditory spatial cue. Nature 430:682–686.

Heffner HE (1997) The role of macaque auditory cortex in sound localization. Acta Otolaryngol Suppl 532:22–27.

Heffner HE, Heffner RS (1990) Effect of bilateral auditory cortex lesions on sound localization in Japanese macaques. J Neurophysiol 64:915–931.

Imig TJ, Irons WA, Samson FR (1990) Single-unit selectivity to azimuthal direction and sound pressure level of noise bursts in cat high-frequency primary auditory cortex. J Neurophysiol 63:1448–1466.

Jenison RL, Reale RA (2003) Likelihood approaches to sensory coding in auditory cortex. Network 14:83–102.

Jiang H, Lepore F, Poirier P, Guillemot JP (2000) Responses of cells to sta-

tionary and moving sound stimuli in the anterior ectosylvian cortex of cats. Hear Res 139:69–85.
Jiang W, Jiang H, Stein BE (2002) Two corticotectal areas facilitate multisensory orientation behavior. J Cogn Neurosci 14:1240–1255.
Kavanagh GL, Kelly JB (1987) Contribution of auditory cortex to sound localization by the ferret (*Mustela putorius*). J Neurophysiol 57:1746–1766.
Keller CH, Hartung K, Takahashi TT (1998) Head-related transfer functions of the barn owl: measurement and neural responses. Hear Res 118:13–34.
King AJ (1993) The Wellcome prize lecture. A map of auditory space in the mammalian brain: neural computation and development. Exp Physiol 78:559–590.
King AJ, Palmer AR (1983) Cells responsive to free-field auditory stimuli in guinea-pig superior colliculus: distribution and response properties. J Physiol (Lond) 342:361–381.
Korte M, Rauschecker JP (1993) Auditory spatial tuning of cortical neurons is sharpened in cats with early blindness. J Neurophysiol 70:1717–1721.
Lomber SG, Malhotra S, Hall AJ (2007) Functional specialization in nonprimary auditory cortex of the cat: areal and laminar contributions to sound localization. Hear Res 229:31–45.
Malhotra S, Hall AJ, Lomber SG (2004) Cortical control of sound localization in the cat: unilateral cooling deactivation of 19 cerebral areas. J Neurophysiol 92:1625–1643.
May BJ, Huang AY (1996) Sound orientation behavior in cats: I. Localization of broadband noise. J Acoust Soc Am 100:1059–1069.
McAlpine D, Grothe B (2003) Sound localization and delay lines—do mammals fit the model? Trends Neurosci 26:347–350.
McAlpine D, Jiang D, Palmer AR (2001) A neural code for low-frequency sound localization in mammals. Nat Neurosci 4:396–401.
Meredith MA, Clemo HR (1989) Auditory cortical projection from the anterior ectosylvian sulcus (Field AES) to the superior colliculus in the cat: an anatomical and electrophysiological study. J Comp Neurol 289:687–707.
Mickey BJ, Middlebrooks JC (2003) Representation of auditory space by cortical neurons in awake cats. J Neurosci 23:8649–8663.
Middlebrooks J, Knudsen E (1984) A neural code for auditory space in the cat's superior colliculus. J Neurosci 4:2621–2634.
Middlebrooks JC, Pettigrew JD (1981) Functional classes of neurons in primary auditory cortex of the cat distinguished by sensitivity to sound location. J Neurosci 1:107–120.
Middlebrooks JC, Clock AE, Xu L, Green DM (1994) A panoramic code for sound location by cortical neurons. Science 264:842–844.
Middlebrooks JC, Xu L, Eddins AC, Green DM (1998) Codes for sound-source location in nontonotopic auditory cortex. J Neurophysiol 80:863–881.
Moshitch D, Las L, Ulanovsky N, Bar-Yosef O, Nelken I (2006) Responses of neurons in primary auditory cortex (A1) to pure tones in the halothane-anesthetized cat. J Neurophysiol 95:3756–3769.
Mrsic-Flogel TD, King AJ, Jenison RL, Schnupp JW (2001) Listening through different ears alters spatial response fields in ferret primary auditory cortex. J Neurophysiol 86:1043–1046.
Mrsic-Flogel TD, Schnupp JW, King AJ (2003) Acoustic factors govern developmental sharpening of spatial tuning in the auditory cortex. Nat Neurosci 6:981–988.
Nelken I, Chechik G, Mrsic-Flogel TD, King AJ, Schnupp JW (2005) Encoding stimulus information by spike numbers and mean response time in primary auditory cortex. J Comput Neurosci 19:199–221.
Poirier P, Jiang H, Lepore F, Guillemot JP (1997) Positional, directional and speed selectivities in the primary auditory cortex of the cat. Hear Res 113:1–13.
Rajan R, Aitkin LM, Irvine DR, McKay J (1990) Azimuthal sensitivity of neurons in primary auditory cortex of cats. I. Types of sensitivity and the effects of variations in stimulus parameters. J Neurophysiol 64:872–887.
Rice JJ, May BJ, Spirou GA, Young ED (1992) Pinna-based spectral cues for sound localization in cat. Hearing Res 58:132–152.
Rice JJ, Young ED, Spirou GA (1995) Auditory-nerve encoding of pinna-based spectral cues: rate representation of high-frequency stimuli. J Acoust Soc Am 97:1764–1776.
Schnupp JW, King AJ (1997) Coding for auditory space in the nucleus of the brachium of the inferior colliculus in the ferret. J Neurophysiol 78:2717–2731.
Schnupp JW, Mrsic-Flogel TD, King AJ (2001) Linear processing of spatial cues in primary auditory cortex. Nature 414:200–204.
Sokal RR, Rohlf FJ (1995) Biometry: the principles and practice of statistics in biological research, Ed 3. New York: W. H. Freeman.
Stecker GC, Mickey BJ, Macpherson EA, Middlebrooks JC (2003) Spatial sensitivity in field PAF of cat auditory cortex. J Neurophysiol 89:2889–2903.
Stecker GC, Harrington IA, Middlebrooks JC (2005a) Location coding by opponent neural populations in the auditory cortex. PLoS Biol 3:e78.
Stecker GC, Harrington IA, Macpherson EA, Middlebrooks JC (2005b) Spatial sensitivity in the dorsal zone (area DZ) of cat auditory cortex. J Neurophysiol 94:1267–1280.
Sterbing SJ, Hartung K, Hoffmann KP (2003) Spatial tuning to virtual sounds in the inferior colliculus of the guinea pig. J Neurophysiol 90:2648–2659.
Xu L, Furukawa S, Middlebrooks JC (1998) Sensitivity to sound-source elevation in nontonotopic auditory cortex. J Neurophysiol 80:882–894.
Yin TC (2002) Neural mechanisms of encoding binaural localization cues in the auditory brainstem. In: Integrative functions in the mammalian auditory pathway (Oertel D, Fay RR, Popper AN, eds), pp 99–159. New York: Springer.
Young ED, Rice JJ, Tong SC (1996) Effects of pinna position on head-related transfer functions in the cat. J Acoust Soc Am 99:3064–3076.